Prompt photons + jet in DIS

P. Bussey, O. Hlushchenko,

D. Saxon, I. Skillicorn

ZEUS collaboration meeting
23 March 2016

Physics overview

- Kinematics:
  - $Q^2 = -q^2$ – virtuality
  - $y = \frac{P \cdot q}{P \cdot l}$ – inelasticity
  - $x = \frac{Q^2}{2P \cdot q}$ – longitudinal momentum fraction carried by the incoming parton

Electron/Positrons: 27.5 GeV
Protons: 920 GeV
Luminosity of ~ 326 pb^{-1}

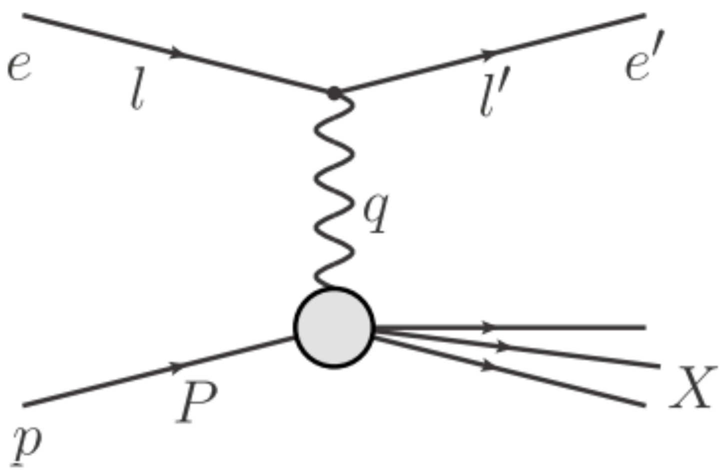

Data
- 0405e, 06e, 0607p

MC
- PYTHIA (signal)
- ARIADNE (background)

Prompt photons

- Photons which are produced promptly in the collision - **before quarks and gluons form hadrons and before those hadrons decay**
- High transverse energy final state photons (E_T^{γ})
- Isolated state:
  - no tracks within $\Delta R(\eta, \varphi) = 0.2$ cone around the photon candidate
  - photon candidate in jet has >=90% of jet energy

QQ - photons

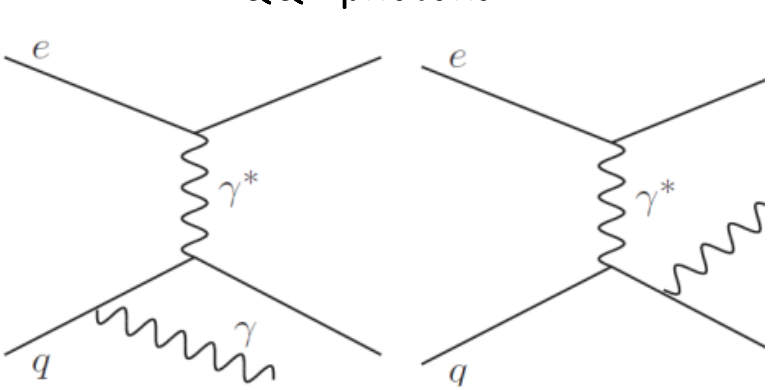

prompt photons are emitted from a quark as part of a QCD process (QQ photons)

LL - photons

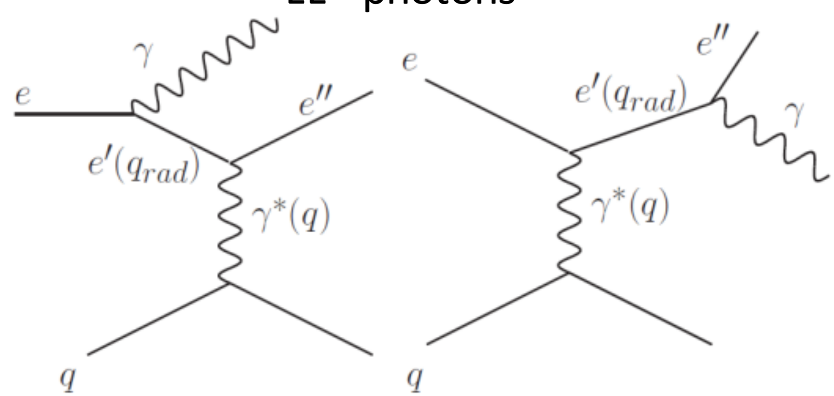

photon is radiated from an incoming or outgoing lepton (LL photons)

Event selection

- DIS selection
  - $10 < Q^2_{el} < 350\ GeV^2$
  - Electron cuts:
    - $E_{e,corr} > 10\ GeV$
    - $140^o < \theta_{el} < 180^o$
    - $|X| < 14.8, cm$
    - $|Y| < 14.8, cm$
- Prompt photon selection
  - $4 < E_T^{\gamma} < 15, GeV$
  - $-0.7 < \eta_{\gamma} < 0.9$
  - $E_{\gamma} \div E_{jet\ with\ \gamma} > 0.9$
  - $\Delta R < 0.2$ – no tracks
  - $E_{EMC} \div (E_{EMC} + E_{HAC})$
- Jet selection (zufos used)
  - $E_T^{jet} > 2.5, GeV$
  - $-1.5 < \eta_{jet} < 1.8$
  - Use jet with $E_{T,max}^{jet}$
- Cleaning
  - Triggers
    - SPP02 for 0405e
    - SPP09 for 06e, 0607p
  - $|Z_{vtx}| < 40, cm$
  - $35 < E - p_z < 65, GeV$
  - Number of vertex tracks not in RCAL > 1

Jet reconstruction

- *Electron* is not used in jet finding
- k_T-clustering alg. from *KtJet* is used (radius parameter R=1)
- Jet which is recognized as containing the photon candidate is excluded
- Highest-E_T^{jet} that does not contain the photon candidate and passes the cuts is treated accompanying hadronic jet

New studied observables

- $x_\gamma = \frac{\sum_{jet,\gamma}(E-p_z)}{2y_{Bj}E_e}$
- $x_p = \frac{\sum_{jet,\gamma}(E+p_z)}{2E_p}$
- $\Delta\eta_{\gamma,jet} = \eta_{jet} - \eta_\gamma$
- $\Delta\varphi_{\gamma,jet} = \varphi_{jet} - \varphi_\gamma$
- $\Delta\eta_{\gamma,e} = \eta_e - \eta_\gamma$
- $\Delta\varphi_{e,\gamma} = \varphi_e - \varphi_\gamma$

Similar kind of analysis was previously done for photoproduction (Q^2<1) for variables $\Delta\eta$, $\Delta\psi$, x_γ, x_p

What was done:

- Moved to new fitting region – excluding the first bin from the fit
- Corrected signal shape
- Studied new ways of doing the fit
- Recalculated and compared new cross sections

Signal extraction

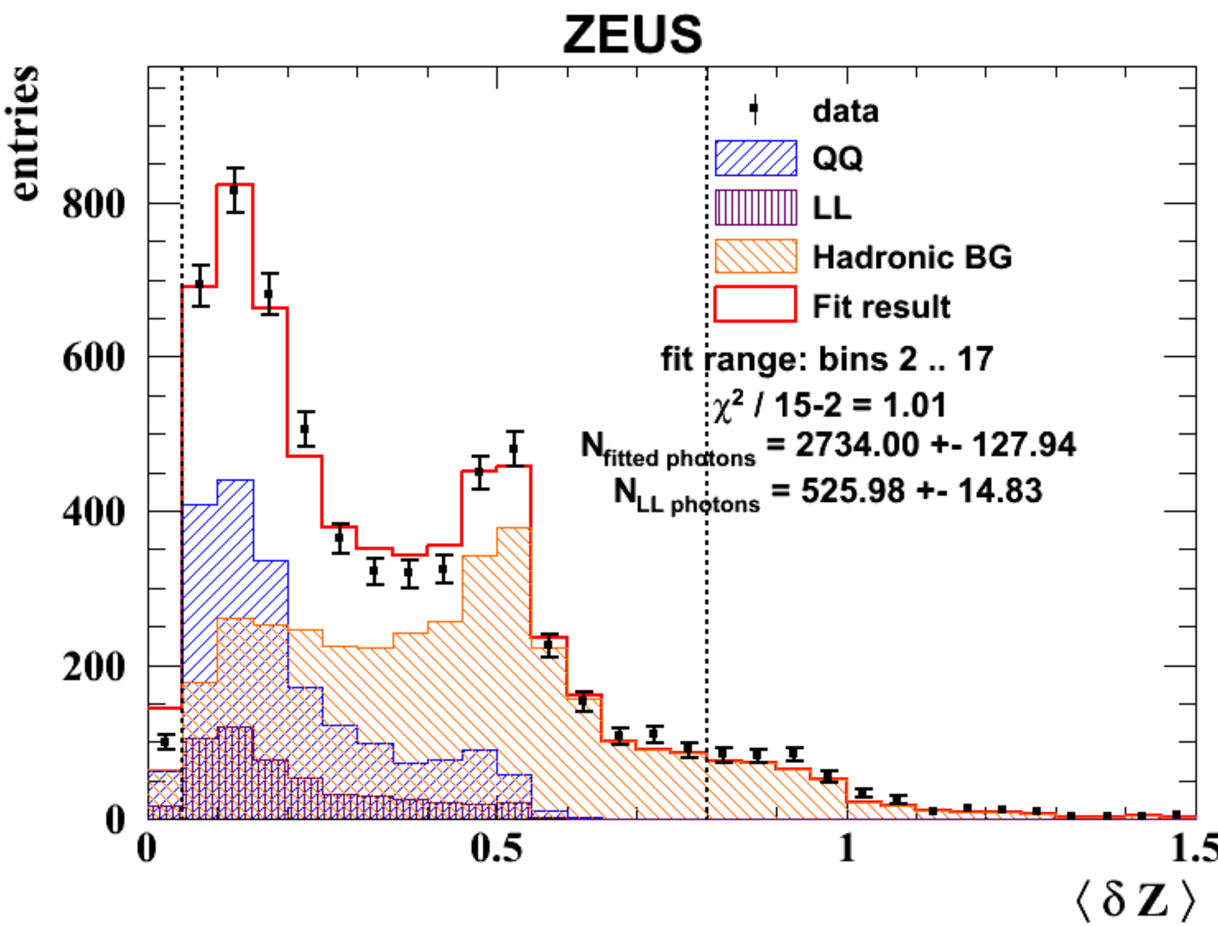

Energy-weighted mean width of the electromagnetic shower(cluster) in calorimeter relative to its centroid:

$$\langle \delta Z \rangle = \frac{\sum_{zufo} |z_i - z_{cluster}| \cdot E_i}{l_{cell} \sum E_i}$$

Number of fitted photons increased compared to 2440±60*. This is mostly due to changing the fitting region.

*ZEUS Collaboration, H. Abramowicz et al., Phys. Lett. B 715 (2012) 88

Signal-shape correction

- The fit became better overall
- Number of fitted photons decreased to 2734
- For DVCS, the deviation between the MC and data is confined to the peak of the distribution therefore only 3 bins of the signal are corrected.

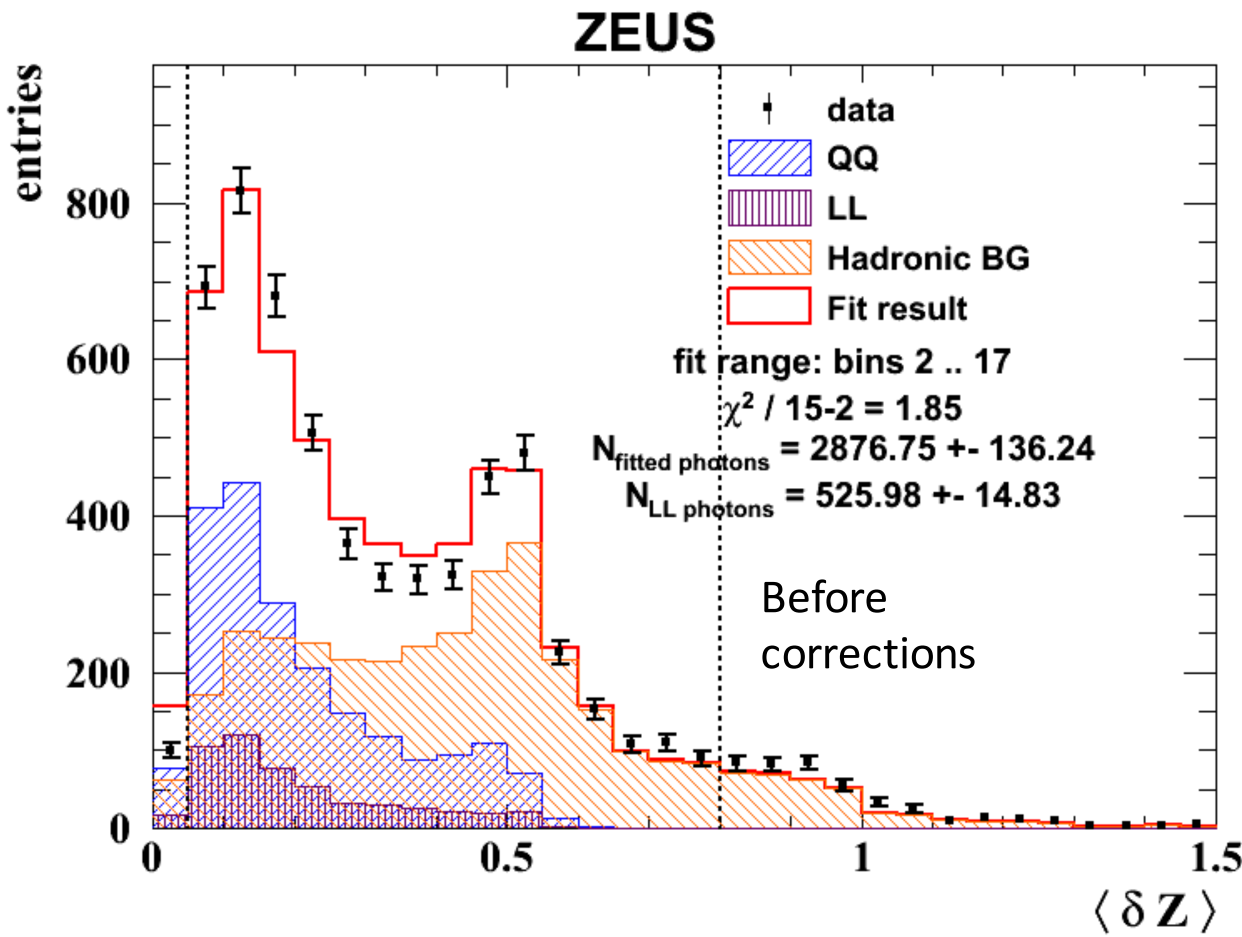

See DVCS plots on http://www.ppe.gla.ac.uk/~skilli/photonjet.html

Acceptance

$$Acc = \frac{N_{detector\ level}}{N_{true\ level}}$$

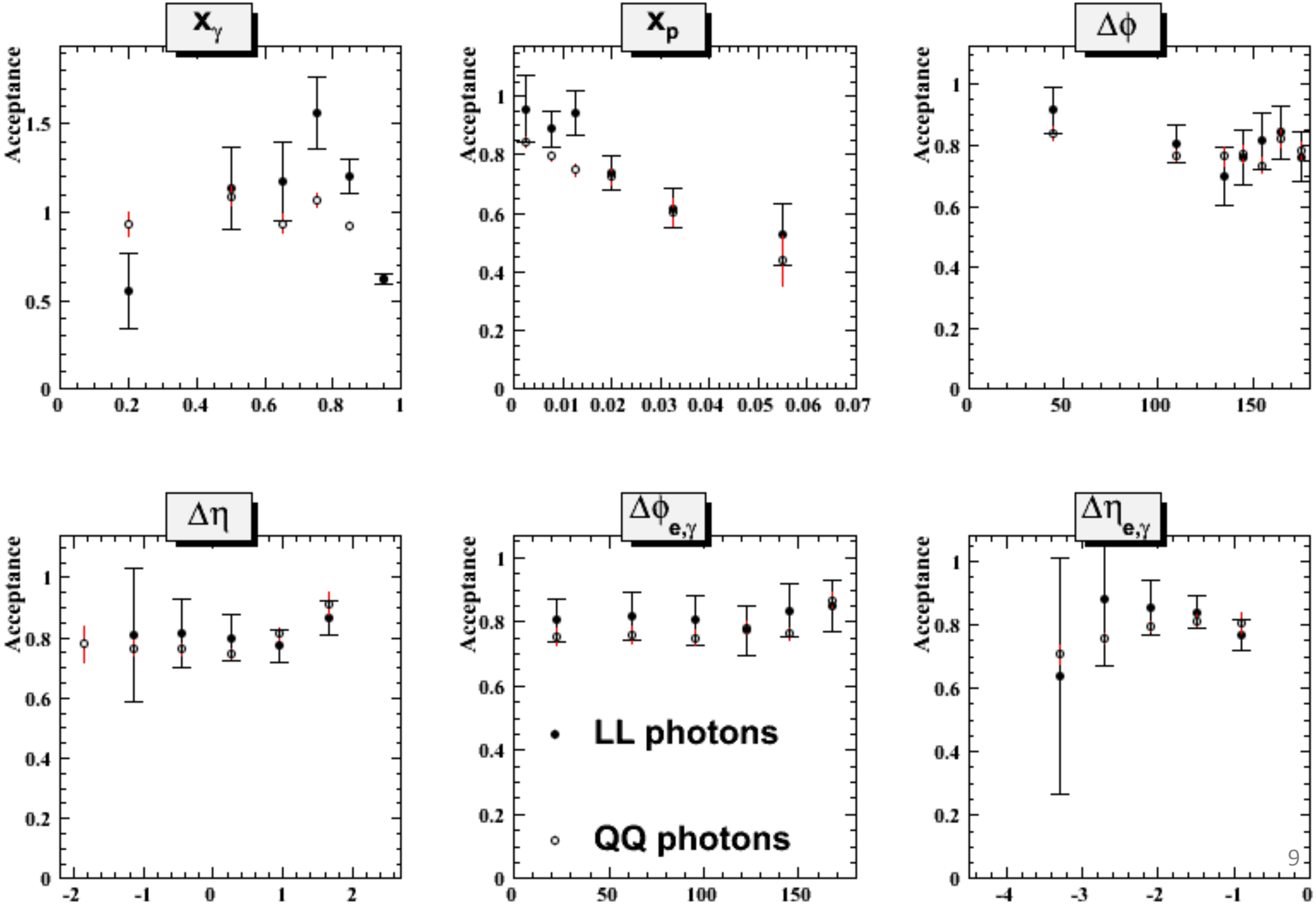

Purity

$$\text{Pur} = \frac{N_{true\ \&\&\ detector\ level}}{N_{detector\ level}}$$

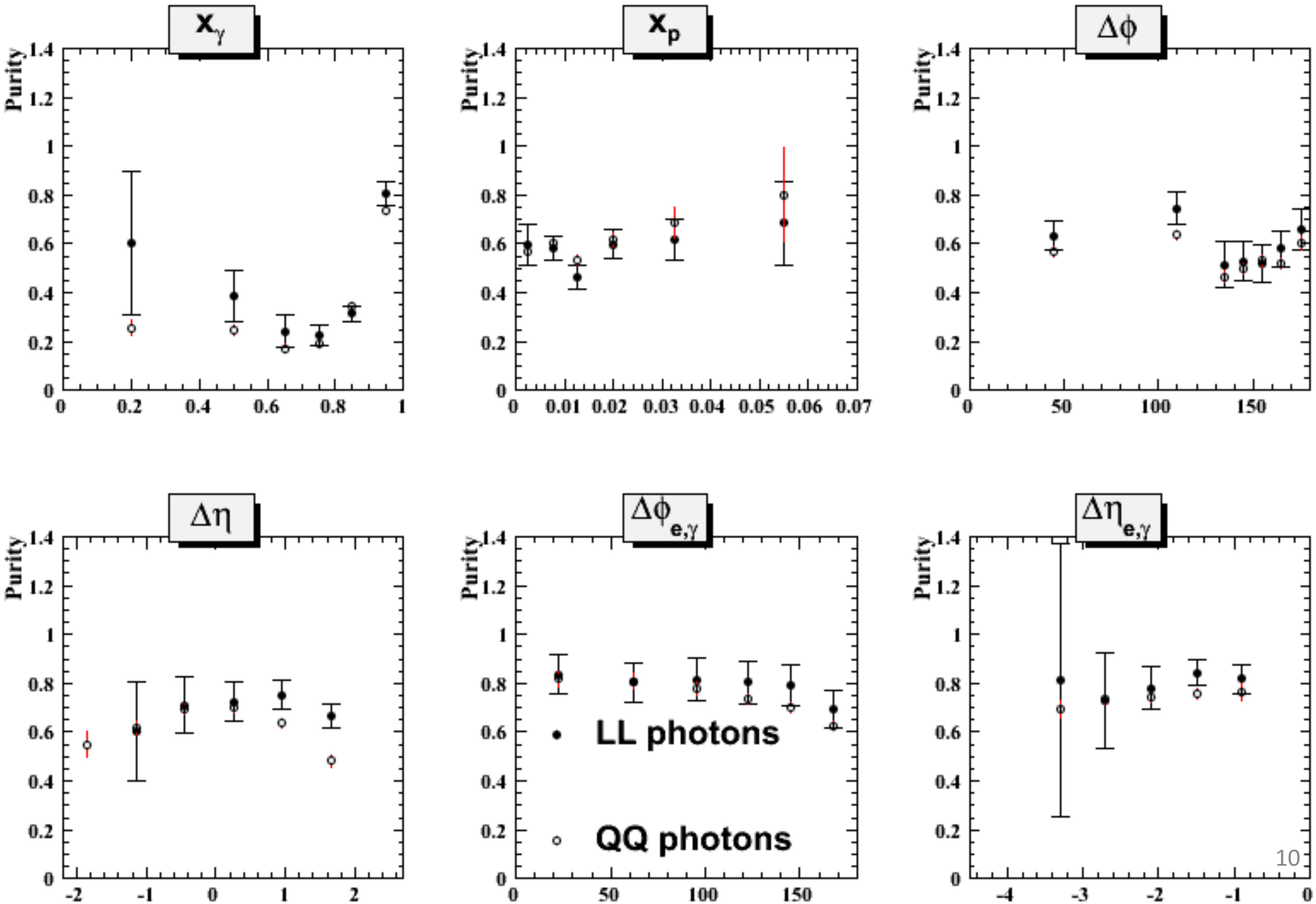

Systematics uncertainties

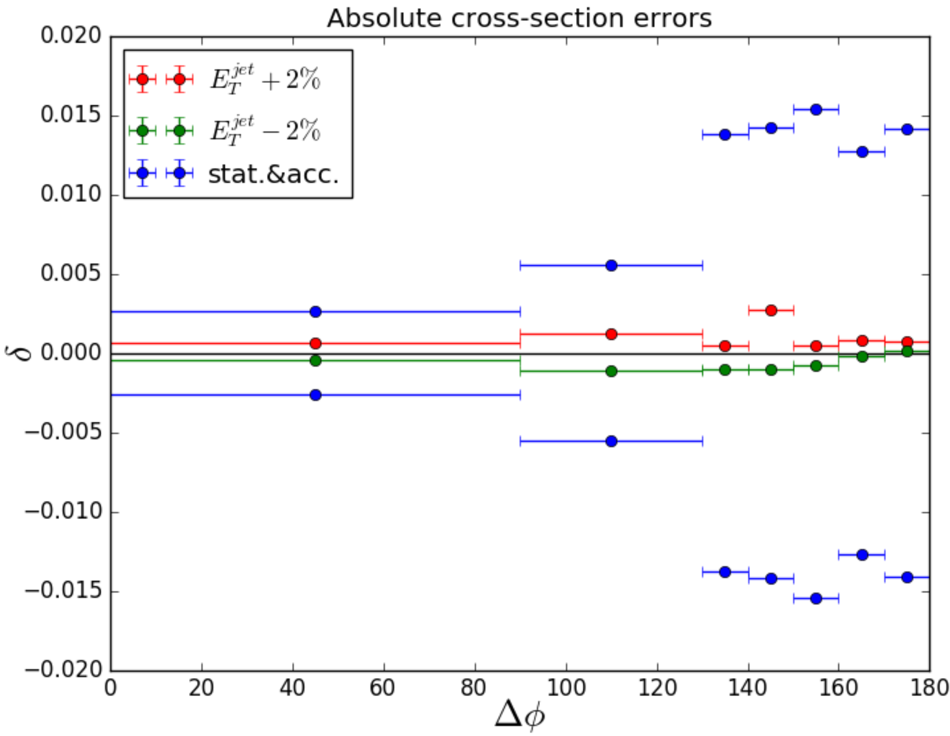

- Before applying cuts for the event selection the values of such variables as:
  - E_γ - energy of the photon
  - E_{jet}- energy of the jet
  - E_e- energy of the electron

are corrected to $\pm 2\%$ and the cross sections are recalculated (one by one, both for MC and Data)

- The obtained CS are then compared to one we calculated previously without any corrections

Uncertainties

- Uncertanties sources:
  - δLuminosity – neglected
  - δN – statistical errors on QQ and LL MC sampes
  - δacc – acceptance errors
  - δa – errors of found fit parameter
- Typical mean statistical uncertainty is 12-13% with maximum 26% for first bin of x_γ and last bin of x_p
- Typical mean systematic uncertainty is 9-10% with maximum 50% in last bin of x_p

Cross sections calculation

- For a given observable Y , the production cross section:

$$\frac{d\sigma}{dY} = \frac{N(\gamma_{QQ})}{A_{QQ} \cdot \mathcal{L} \cdot \Delta Y} + \frac{d\sigma_{LL}^{MC}}{dY}$$

$N(\gamma_{QQ})$ - number of QQ photons extracted from the fit,

ΔY - bin width,

$\mathcal{L}$ - total integrated luminosity,

$\frac{d\sigma_{LL}^{MC}}{dY}$- cross section for LL photons

A_{QQ} - ratio of the number of events reconstructed to those generated in a given bin

Comparison with article

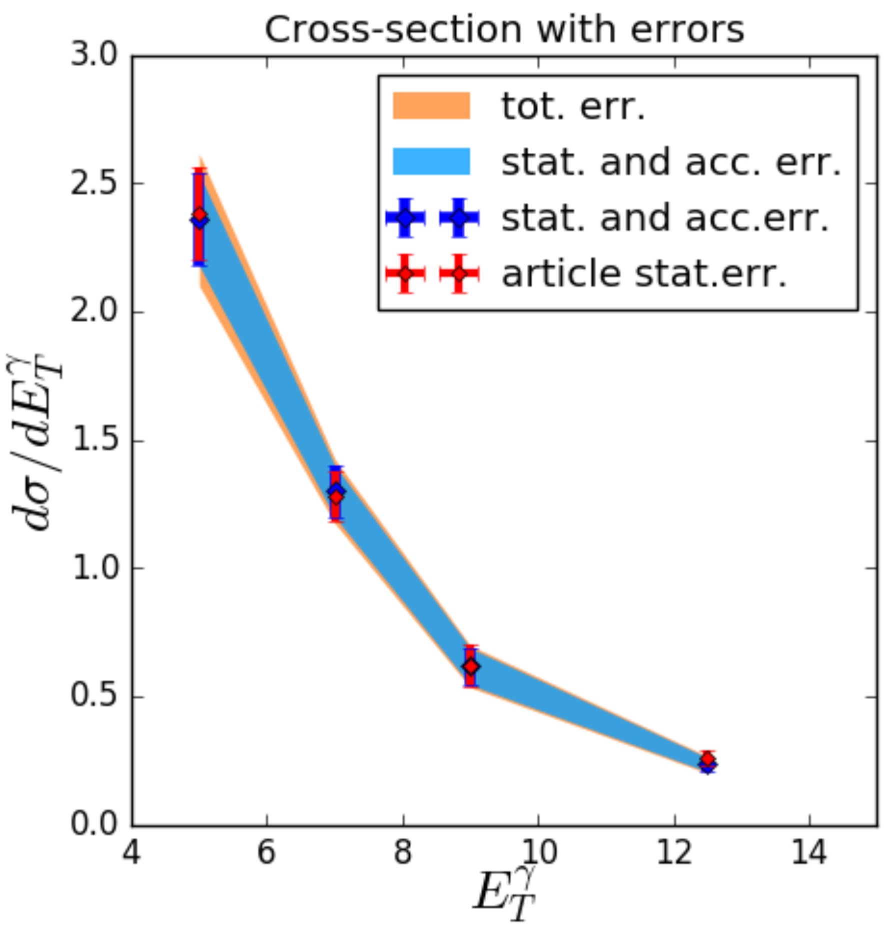

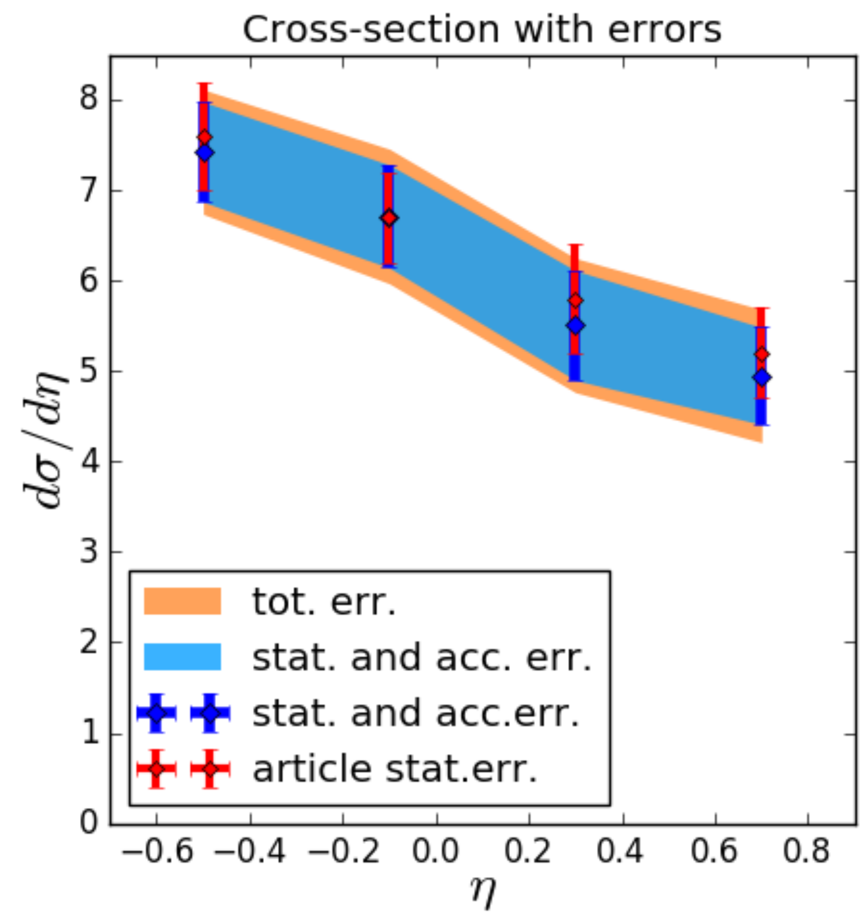

Theory

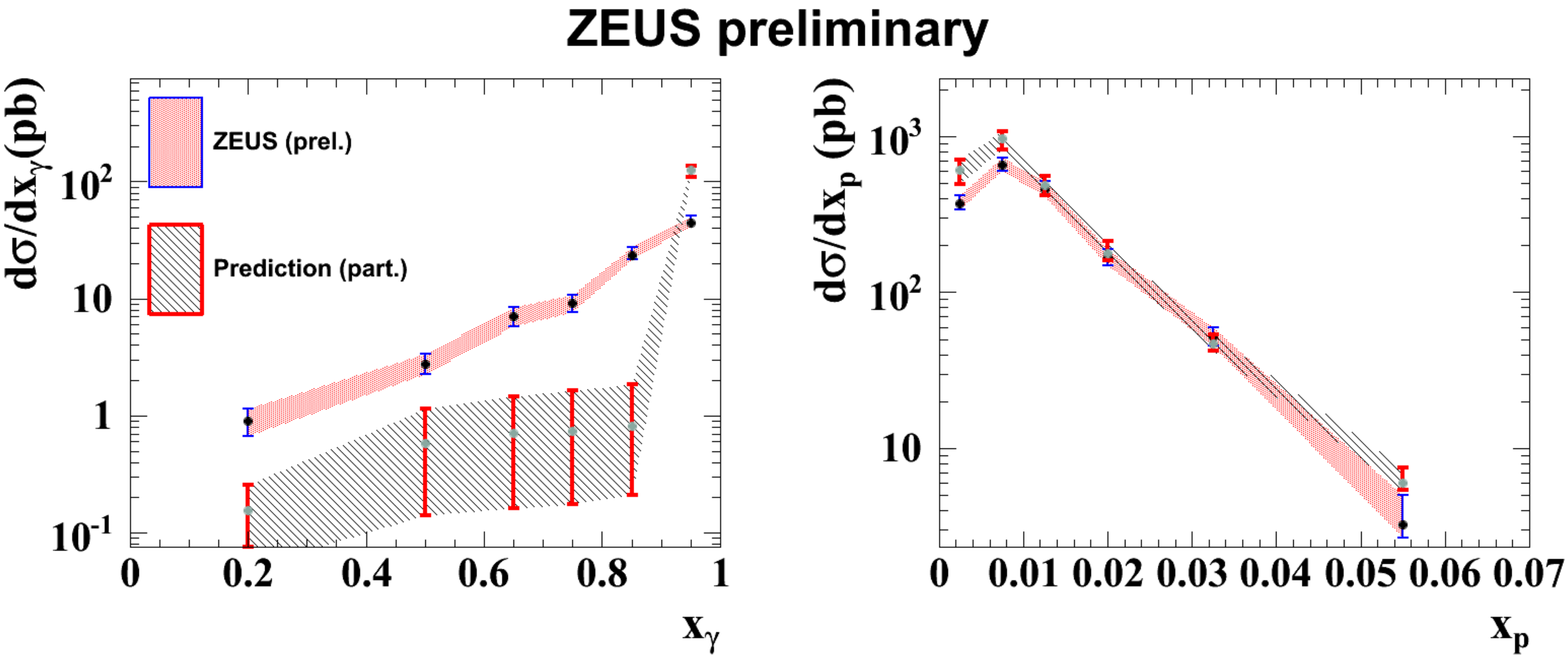

ZEUS preliminary
ZEUS (prel.)
Prediction (part.)
dσ/dx_γ(pb)
10^2
10
1
10^-1
0
0.2
0.4
0.6
0.8
1
x_γ
dσ/dx_p (pb)
10^3
10^2
10
0
0.01
0.02
0.03
0.04
0.05
0.06
0.07
x_p

Theory

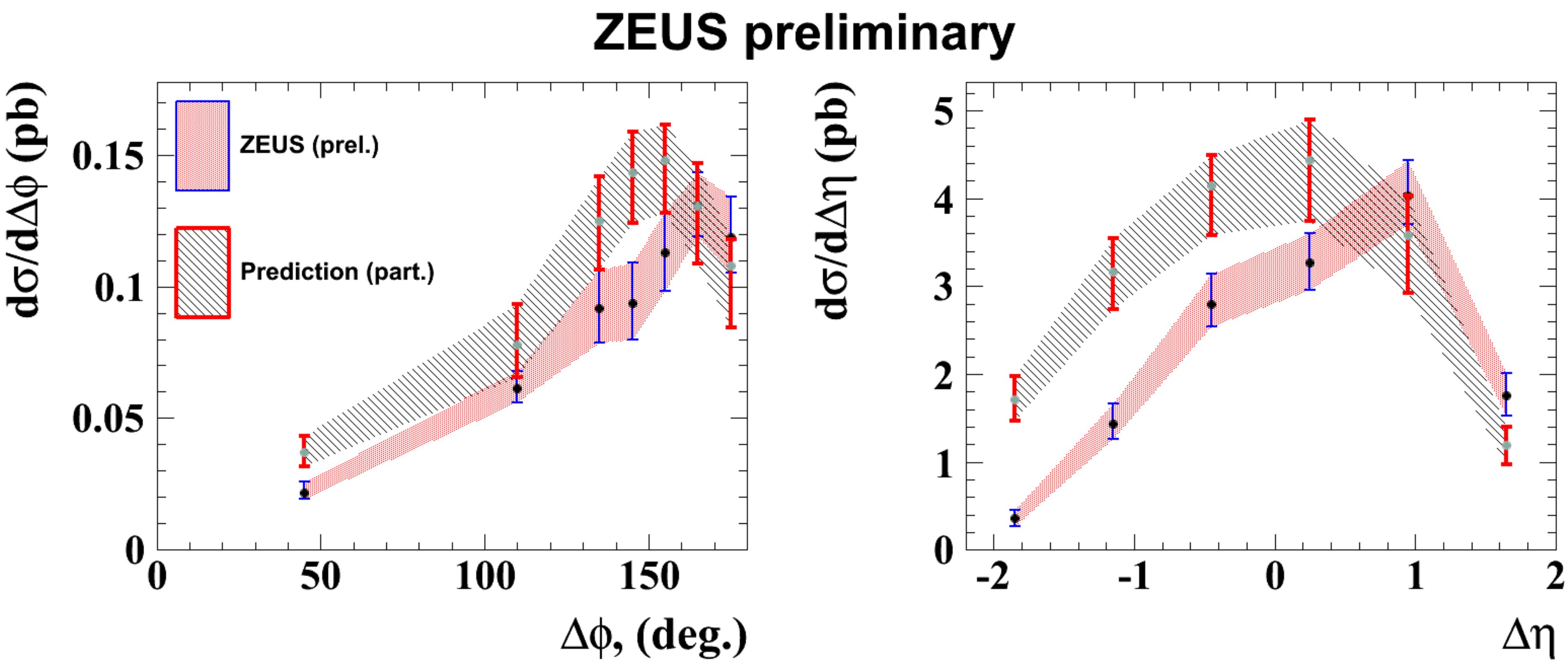
ZEUS preliminary
ZEUS (prel.)
Prediction (part.)
dσ/dΔφ (pb)
0.15
0.1
0.05
0
0
50
100
150
Δφ, (deg.)
dσ/dΔη (pb)
5
4
3
2
1
0
-2
-1
0
1
2
Δη

Theory

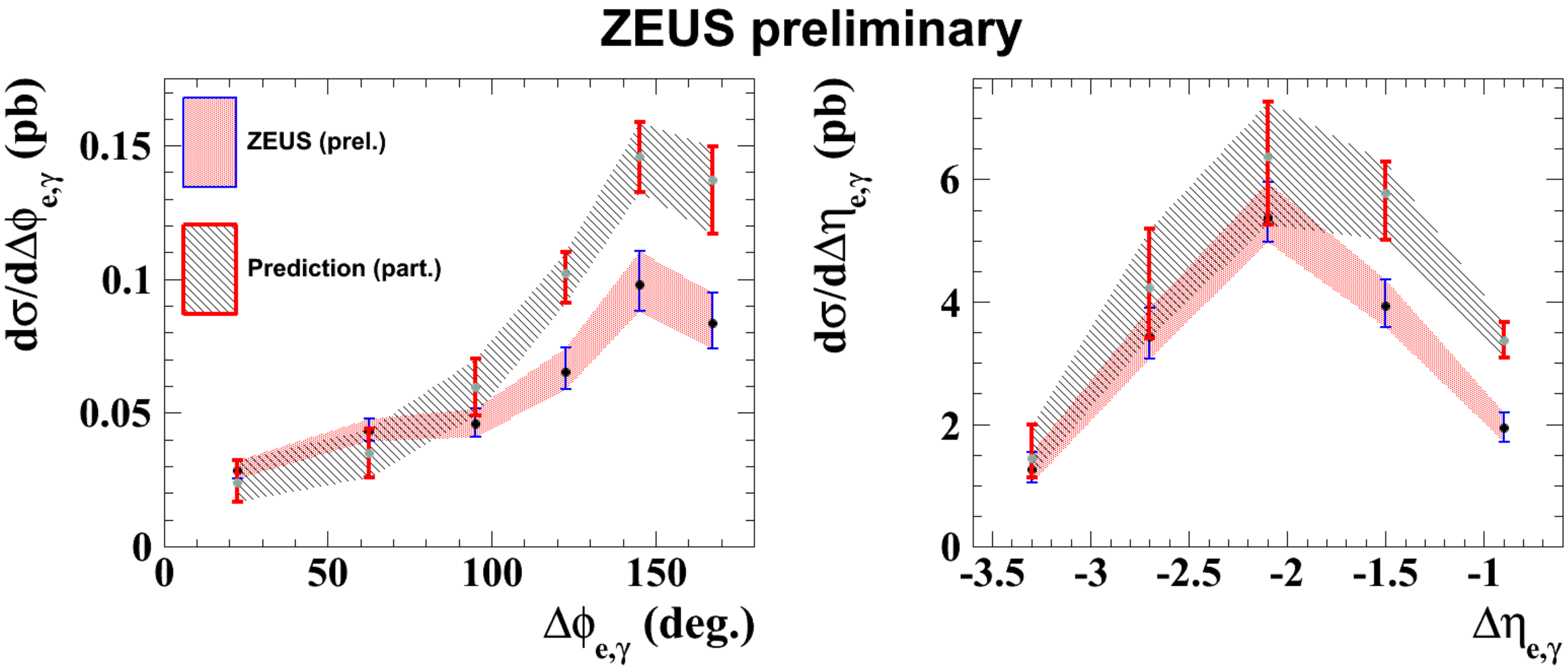

ZEUS preliminary
ZEUS (prel.)
Prediction (part.)
dσ/dΔφe,γ (pb)
0.15
0.1
0.05
0
0
50
100
150
Δφe,γ (deg.)
dσ/dΔηe,γ (pb)
6
4
2
0
-3.5
-3
-2.5
-2
-1.5
-1
Δηe,γ

Preliminary

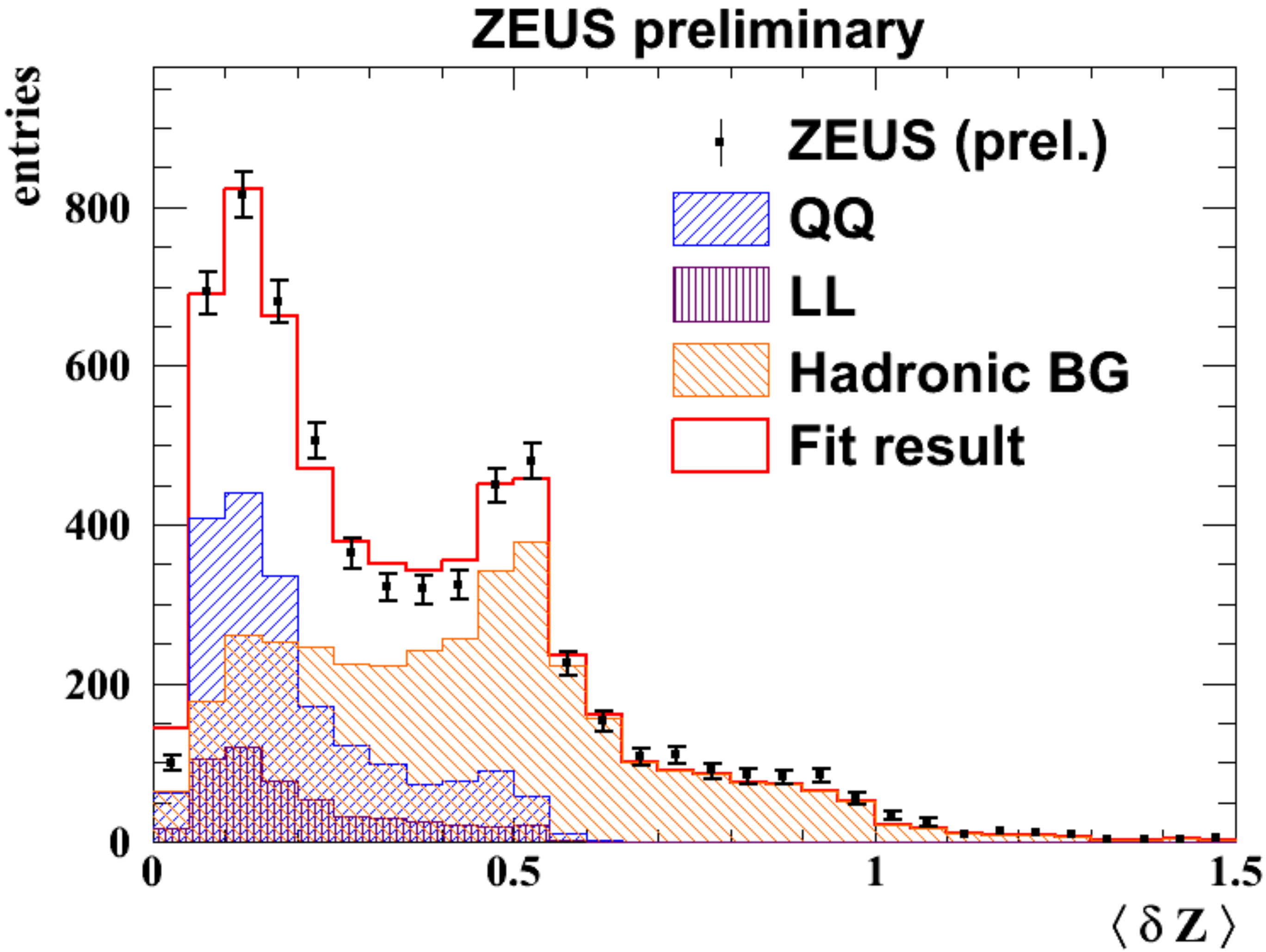

Preliminary

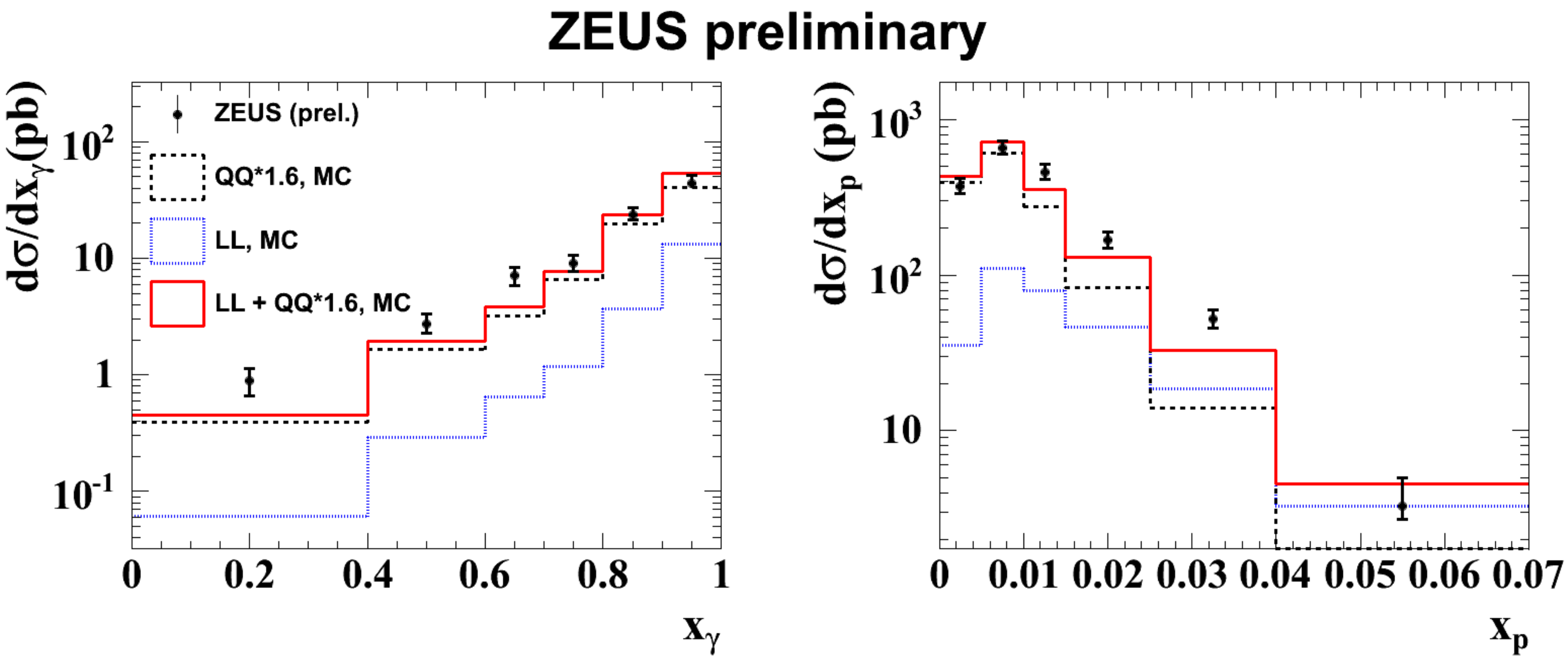

Preliminary

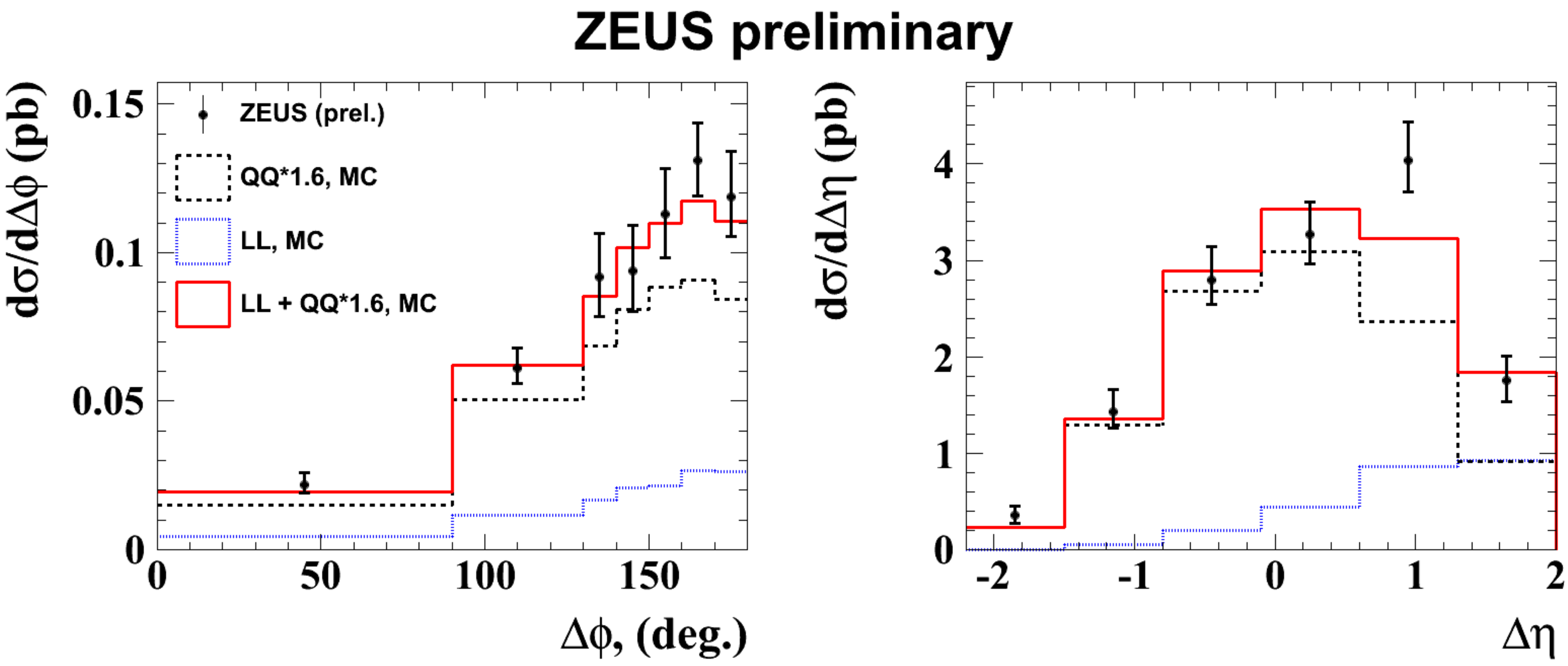

Preliminary

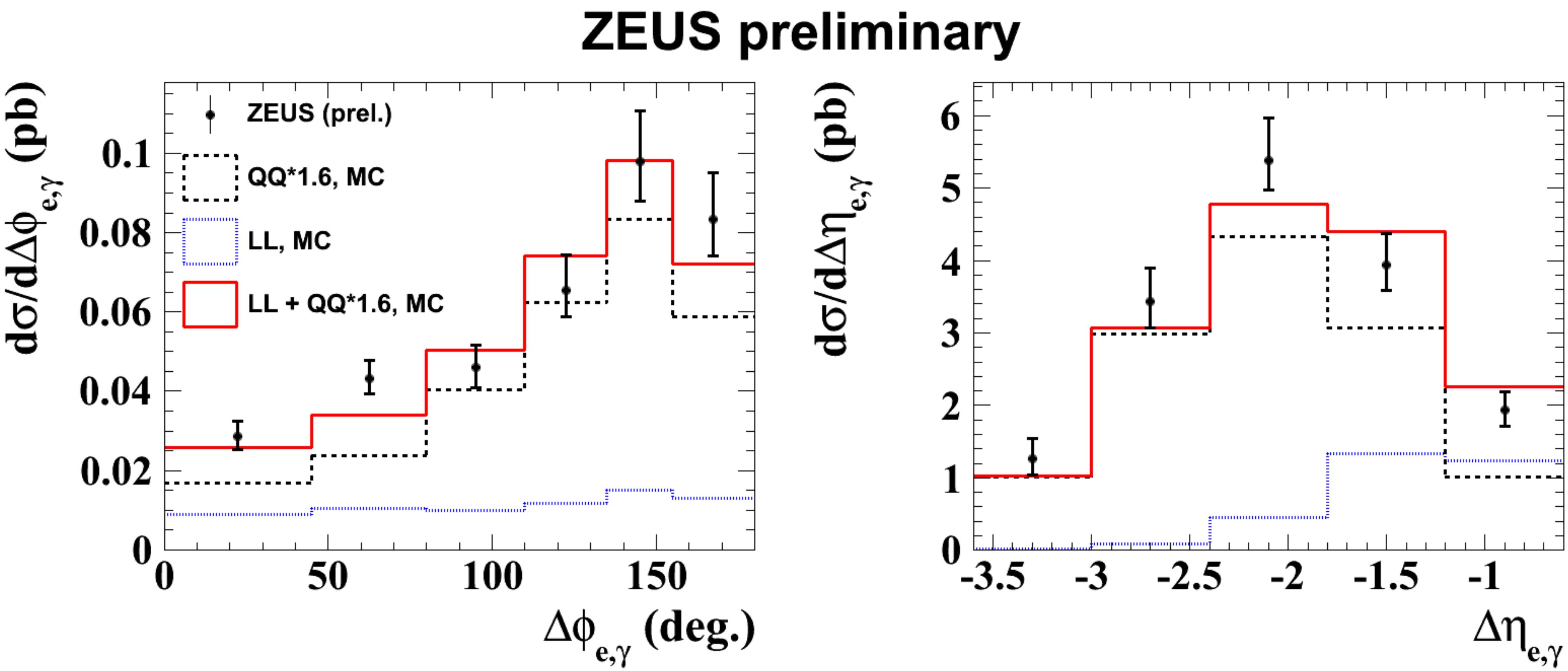

Conclusions

- We confirmed the previous published paper results
- Cross sections were built in different regions of new observables of interest e.g. $\Delta\eta$, $\Delta\psi$, $\Delta\psi_{e,\gamma,}$, x_{γ}, x_{p}, similar as it was done for photoproduction
- We have asked the theoretical group for more calculations and we wait for their replies

Appendix. Paper CS vs New code(same constrains)

E_T^γ range (GeV)	$\frac{d\sigma}{dE_T^\gamma}$ (pb GeV^{-1})	New CS
4–6	2.38 ± 0.18 (stat.) ± 0.13 (sys.)	2.387730 +- 0.1642(stat.) +- 0.1921(sys.)
6–8	1.28 ± 0.10 (stat.) ± 0.06 (sys.)	1.275860 +- 0.0938(stat.) +- 0.0693(sys.)
8–10	0.62 ± 0.08 (stat.) ± 0.04 (sys.)	0.621169 +- 0.0673(stat.) +- 0.0392(sys.)
10–15	0.26 ± 0.03 (stat.) ± 0.02 (sys.)	0.253476 +- 0.0242(stat.) +- 0.0205(sys.)

η^γ range	$\frac{d\sigma}{d\eta^\gamma}$ (pb)	New CS
−0.7 to −0.3	7.6 ± 0.6 (stat.) ± 0.5 (sys.)	7.630460 +- 0.5508(stat.) +- 0.4702(sys.)
−0.3–0.1	6.7 ± 0.5 (stat.) ± 0.3 (sys.)	6.751080 +- 0.5011(stat.) +- 0.4657(sys.)
0.1–0.5	5.8 ± 0.6 (stat.) ± 0.3 (sys.)	5.857360 +- 0.5171(stat.) +- 0.4662(sys.)
0.5–0.9	5.2 ± 0.5 (stat.) ± 0.4 (sys.)	5.129550 +- 0.5150(stat.) +- 0.5077(sys.)

Q^2 range (GeV^2)	$\frac{d\sigma}{dQ^2}$ (pb GeV^{-2})	New CS
10–20	0.298 ± 0.024 (stat.) ± 0.019 (sys.)	0.296325 +- 0.0230(stat.) +- 0.0236(sys.)
20–40	0.129 ± 0.012 (stat.) ± 0.009 (sys.)	0.131084 +- 0.0109(stat.) +- 0.0107(sys.)
40–80	0.049 ± 0.005 (stat.) ± 0.004 (sys.)	0.049380 +- 0.0049(stat.) +- 0.0050(sys.)
80–150	0.0224 ± 0.0023 (stat.) ± 0.0011 (sys.)	0.022110 +- 0.0021(stat.) +- 0.0015(sys.)
150–350	0.0037 ± 0.0007 (stat.) ± 0.0002 (sys.)	0.003589 +- 0.0006(stat.) +- 0.0001(sys.)

Appendix. Paper CS vs New code(same constrains)

x range	$\frac{d\sigma}{dx}$ (pb)	New CS
0.0002–0.001	4869 ± 334 (stat.) ± 312 (sys.)	4909 +- 316.0841(stat.) +- 375.5895(sys.)
0.001–0.003	1811 ± 139 (stat.) ± 104 (sys.)	1820 +- 129.6690(stat.) +- 125.5547(sys.)
0.003–0.01	278 ± 31 (stat.) ± 13 (sys.)	278 +- 28.7059(stat.) +- 18.7057(sys.)
0.01–0.02	25 ± 7 (stat.) ± 3 (sys.)	24 +- 6.1383(stat.) +- 2.0549(sys.)

E_T^{jet} range (GeV)	$\frac{d\sigma}{dE_T^{jet}}$ (pb GeV^{-1})	New CS
2.5–4	1.40 ± 0.16 (stat.) ± 0.08 (sys.)	1.416630 +- 0.1510(stat.) +- 0.1228(sys.)
4–6	1.19 ± 0.11 (stat.) ± 0.10 (sys.)	1.196730 +- 0.0989(stat.) +- 0.0994(sys.)
6–8	1.01 ± 0.10 (stat.) ± 0.07 (sys.)	1.001290 +- 0.0899(stat.) +- 0.0706(sys.)
8–10	0.74 ± 0.07 (stat.) ± 0.05 (sys.)	0.735747 +- 0.0670(stat.) +- 0.0440(sys.)
10–15	0.32 ± 0.03 (stat.) ± 0.02 (sys.)	0.307470 +- 0.0305(stat.) +- 0.0141(sys.)
15–35	0.031 ± 0.006 (stat.) ± 0.003 (sys.)	0.032217 +- 0.0056(stat.) +- 0.0072(sys.)

η^{jet} range	$\frac{d\sigma}{d\eta^{jet}}$ (pb)	
−1.5 to −0.7	1.53 ± 0.17 (stat.) ± 0.15 (sys.)	1.510500 +- 0.1593(stat.) +- 0.1591(sys.)
−0.7–0.1	2.84 ± 0.25 (stat.) ± 0.19 (sys.)	2.875490 +- 0.2268(stat.) +- 0.2513(sys.)
0.1–0.9	3.91 ± 0.33 (stat.) ± 0.14 (sys.)	3.874260 +- 0.3025(stat.) +- 0.2132(sys.)
0.9–1.8	3.57 ± 0.29 (stat.) ± 0.22 (sys.)	3.609000 +- 0.2696(stat.) +- 0.2471(sys.)

Appendix. Paper CS vs New code(new constrains)

E_T^γ range (GeV)	$\frac{d\sigma}{dE_T^\gamma}$ (pb GeV^{-1})	New CS
4–6	2.38 ± 0.18 (stat.) ± 0.13 (sys.)	2.358670 +- 0.1741(stat.) +- 0.1846(sys.)
6–8	1.28 ± 0.10 (stat.) ± 0.06 (sys.)	1.301010 +- 0.0956(stat.) +- 0.0746(sys.)
8–10	0.62 ± 0.08 (stat.) ± 0.04 (sys.)	0.617637 +- 0.0686(stat.) +- 0.0393(sys.)
10–15	0.26 ± 0.03 (stat.) ± 0.02 (sys.)	0.234739 +- 0.0250(stat.) +- 0.0190(sys.)

η^γ range	$\frac{d\sigma}{d\eta^\gamma}$ (pb)	New CS
−0.7 to −0.3	7.6 ± 0.6 (stat.) ± 0.5 (sys.)	7.428260 +- 0.5212(stat.) +- 0.4112(sys.)
−0.3–0.1	6.7 ± 0.5 (stat.) ± 0.3 (sys.)	6.715560 +- 0.5471(stat.) +- 0.4801(sys.)
0.1–0.5	5.8 ± 0.6 (stat.) ± 0.3 (sys.)	5.508910 +- 0.5930(stat.) +- 0.4276(sys.)
0.5–0.9	5.2 ± 0.5 (stat.) ± 0.4 (sys.)	4.949620 +- 0.5130(stat.) +- 0.5033(sys.)

Q^2 range (GeV^2)	$\frac{d\sigma}{dQ^2}$ (pb GeV^{-2})	New CS
10–20	0.298 ± 0.024 (stat.) ± 0.019 (sys.)	0.294859 +- 0.0241(stat.) +- 0.0224(sys.)
20–40	0.129 ± 0.012 (stat.) ± 0.009 (sys.)	0.117768 +- 0.0118(stat.) +- 0.0085(sys.)
40–80	0.049 ± 0.005 (stat.) ± 0.004 (sys.)	0.049034 +- 0.0049(stat.) +- 0.0055(sys.)
80–150	0.0224 ± 0.0023 (stat.) ± 0.0011 (sys.)	0.022872 +- 0.0022(stat.) +- 0.0015(sys.)
150–350	0.0037 ± 0.0007 (stat.) ± 0.0002 (sys.)	0.004092 +- 0.0006(stat.) +- 0.0001(sys.)

Appendix. Paper CS vs New code(new constrains)

x range	$\frac{d\sigma}{dx}$ (pb)	New CS
0.0002–0.001	4869 ± 334 (stat.) ± 312 (sys.)	4772.700 +- 330.765(stat.) +- 358.1813(sys.)
0.001–0.003	1811 ± 139 (stat.) ± 104 (sys.)	1772.600 +- 134.710(stat.) +- 120.0599(sys.)
0.003–0.01	278 ± 31 (stat.) ± 13 (sys.)	269.4830 +- 30.721(stat.) +- 17.7598(sys.)
0.01–0.02	25 ± 7 (stat.) ± 3 (sys.)	26.1334 +- 5.935(stat.) +- 1.9982(sys.)

$E_T^{\rm jet}$ range (GeV)	$\frac{d\sigma}{dE_T^{\rm jet}}$ (pb GeV^{-1})	New CS
2.5–4	1.40 ± 0.16 (stat.) ± 0.08 (sys.)	1.317900 +- 0.1628(stat.) +- 0.1058(sys.)
4–6	1.19 ± 0.11 (stat.) ± 0.10 (sys.)	1.195660 +- 0.1040(stat.) +- 0.0992(sys.)
6–8	1.01 ± 0.10 (stat.) ± 0.07 (sys.)	0.984009 +- 0.0937(stat.) +- 0.0674(sys.)
8–10	0.74 ± 0.07 (stat.) ± 0.05 (sys.)	0.728794 +- 0.0651(stat.) +- 0.0481(sys.)
10–15	0.32 ± 0.03 (stat.) ± 0.02 (sys.)	0.313586 +- 0.0310(stat.) +- 0.0138(sys.)
15–35	0.031 ± 0.006 (stat.) ± 0.003 (sys.)	0.032861 +- 0.0046(stat.) +- 0.0060(sys.)

$\eta^{\rm jet}$ range	$\frac{d\sigma}{d\eta^{\rm jet}}$ (pb)	New CS
-1.5 to -0.7	1.53 ± 0.17 (stat.) ± 0.15 (sys.)	1.626160 +- 0.1634(stat.) +- 0.1926(sys.)
-0.7–0.1	2.84 ± 0.25 (stat.) ± 0.19 (sys.)	2.978560 +- 0.2364(stat.) +- 0.2631(sys.)
0.1–0.9	3.91 ± 0.33 (stat.) ± 0.14 (sys.)	3.787610 +- 0.3207(stat.) +- 0.1988(sys.)
0.9–1.8	3.57 ± 0.29 (stat.) ± 0.22 (sys.)	3.329450 +- 0.2767(stat.) +- 0.2273(sys.)

Comparison with article

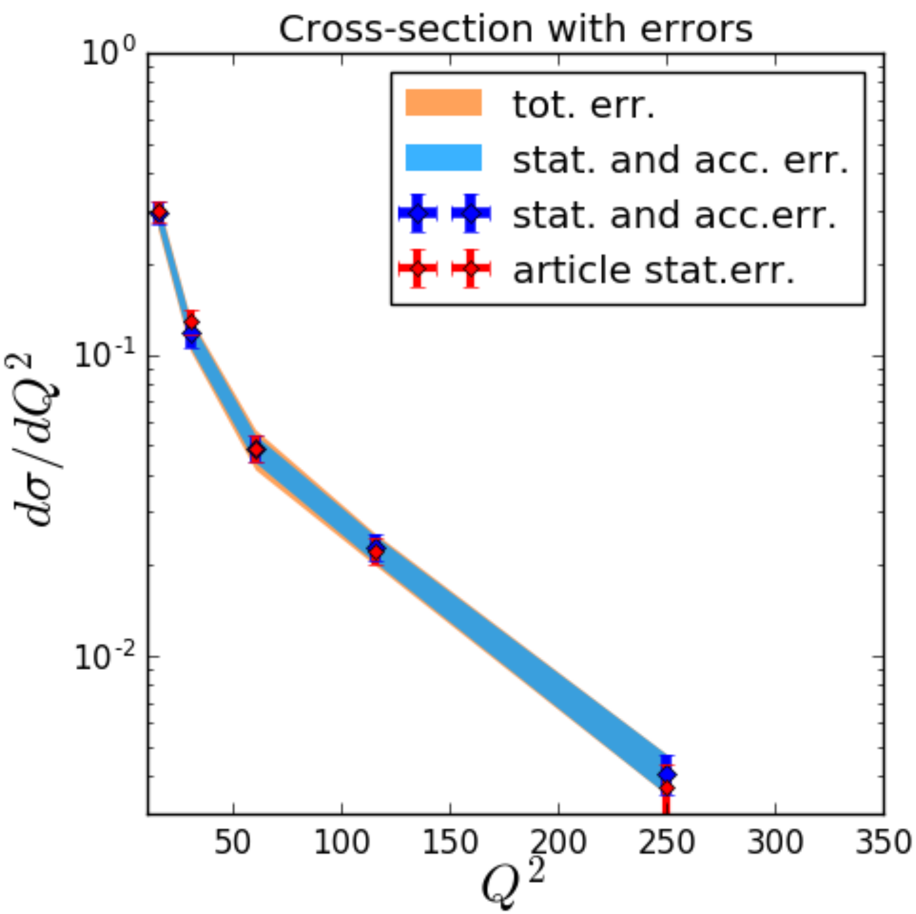

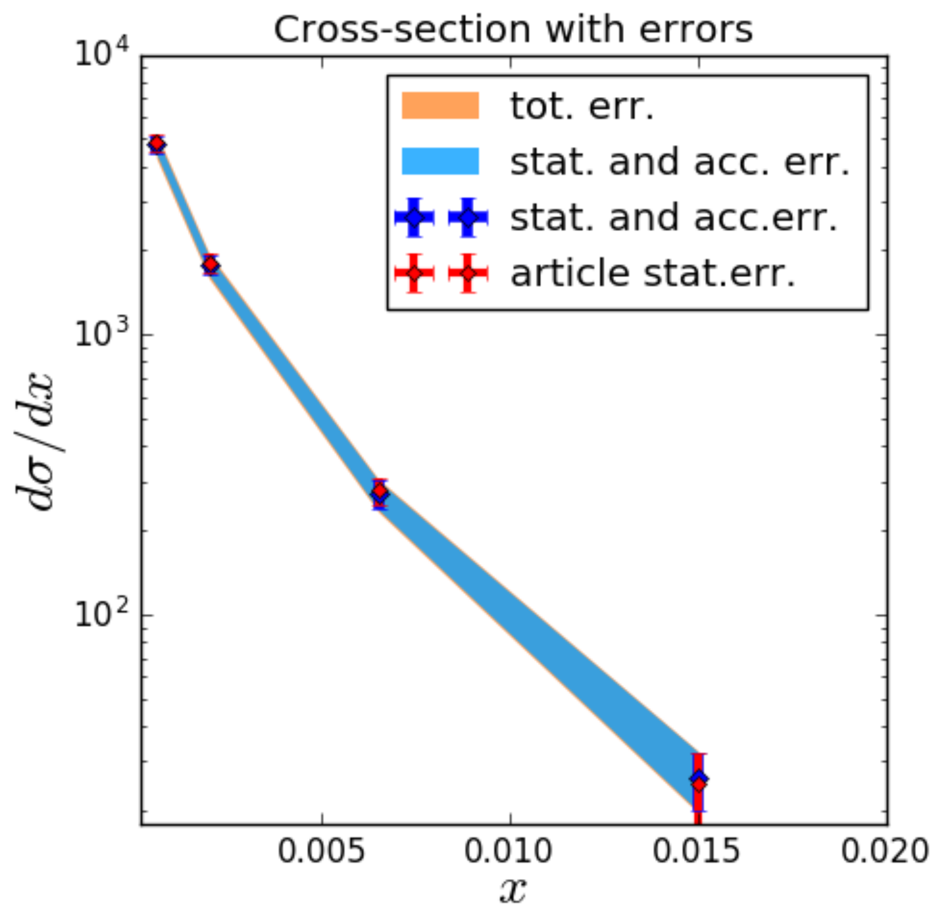

Comparison with article

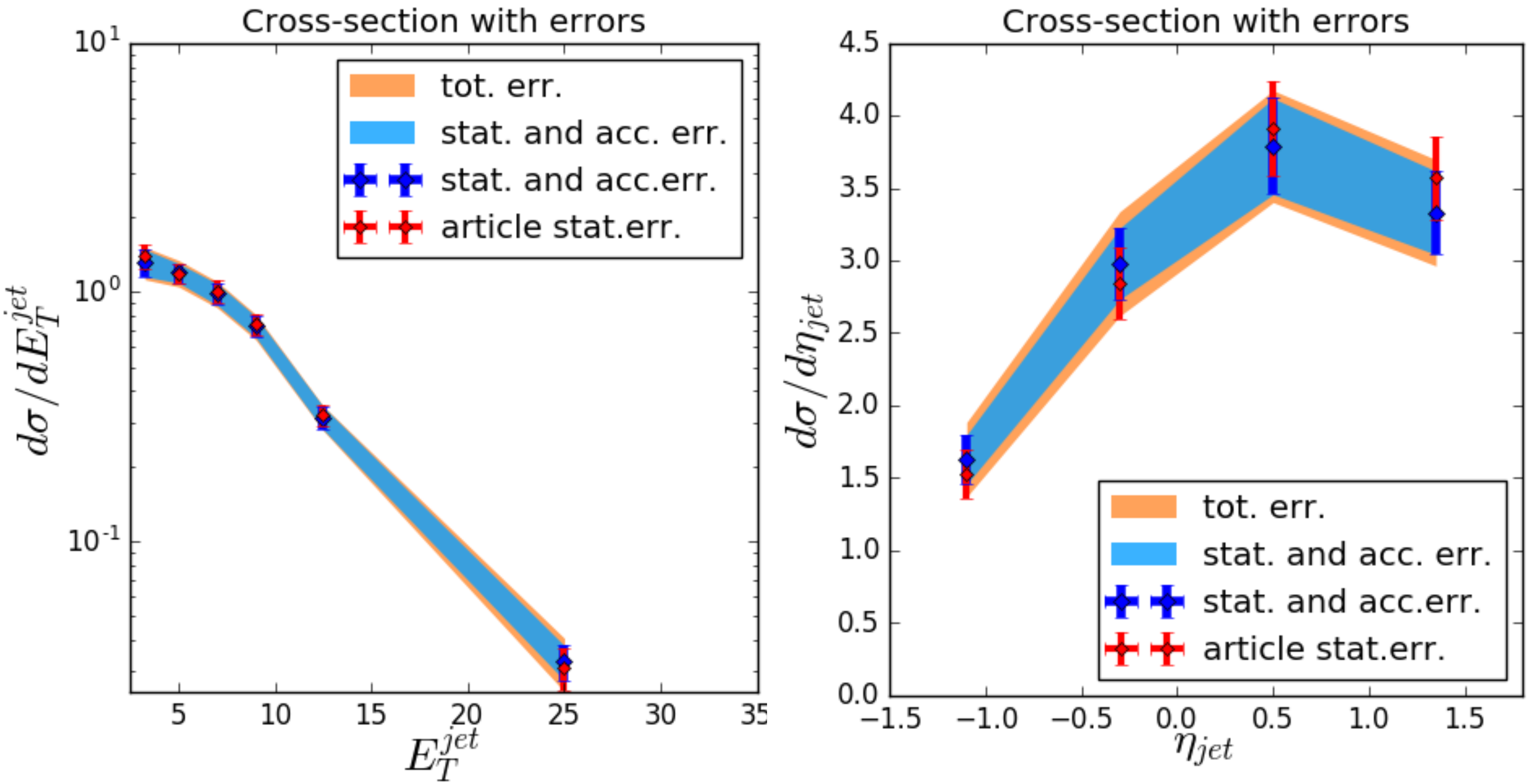

Appendix. Total cross section

- variable E_T^{γ} σ_{tot} = 9.7283 +- 0.4152 pb Prev. paper was 9.86 +/- 0.45 pb
- variable η_{γ} σ_{tot} = 9.84094 +- 0.411581 pb
- variable Q^2 σ_{tot} = 9.68468 +- 0.411113 pb
- variable x σ_{tot} = 9.51108 +- 0.415857 pb
- variable E_T^{jet} σ_{tot} = 10.0189 +- 0.407521 pb
- variable η_{jet} σ_{tot} = 9.71037 +- 0.389135 pb
- variable x_{γ} σ_{tot} = 9.29195 +- 0.331309 pb
- variable x_p σ_{tot} = 9.98807 +- 0.417831 pb
- variable $\Delta\varphi$ σ_{tot} = 9.89287 +- 0.408290 pb
- variable $\Delta\eta$ σ_{tot} = 9.55389 +- 0.371788 pb
- variable $\Delta\varphi^{e,\gamma}$ σ_{tot} = 9.85318 +- 0.391102 pb
- variable $\Delta\eta^{e,\gamma}$ σ_{tot} = 9.57181 +- 0.402304 pb

Appendix. Studied fits

- A bin by bin $min\chi^2$-fitting procedures is done. The minimized functions:
  1. $\boldsymbol{Data - Photons_{MC} * a - Background_{MC} * (1-a)}$
  2. $\boldsymbol{Data - LL_{MC} - QQ_{MC} * a - Background_{MC} * (1-a)}$
  3. $\boldsymbol{Data - QQ_{MC} * a - Background_{MC} * (1-a)}$
  4. $\boldsymbol{Data - QQ_{MC} * a - Background'_{MC} * (1-a)}$
- Number of fitted photons is defined:
  - $\boldsymbol{N = a * Ndata_{,full} * \frac{N_{sg,full}}{N_{sg,fitted}} + NLL_{,full}}$ for (1) and (2)
  - $\boldsymbol{N = a * Ndata_{,full} * \frac{N_{sg,full}}{N_{sg,fitted}}}$ for (3) and (4)

* $\boldsymbol{Background_{MC}}$ - hadronic background

** $\boldsymbol{Background'_{MC}}$ - hadronic background and $\boldsymbol{LL_{MC}}$

*** $\boldsymbol{Photons_{MC}}$ - $\boldsymbol{QQ_{MC}}$ and $\boldsymbol{LL_{MC}}$

Δφ bin-by-bin fit

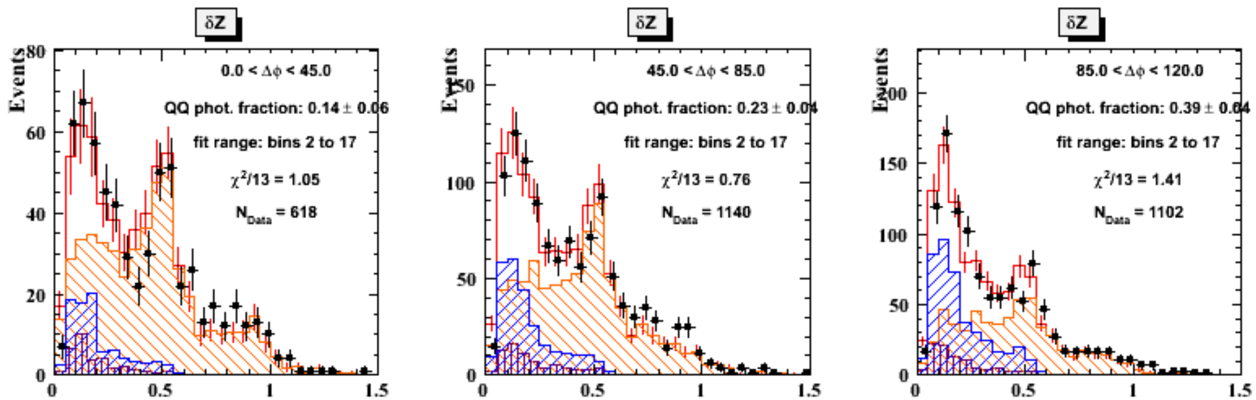

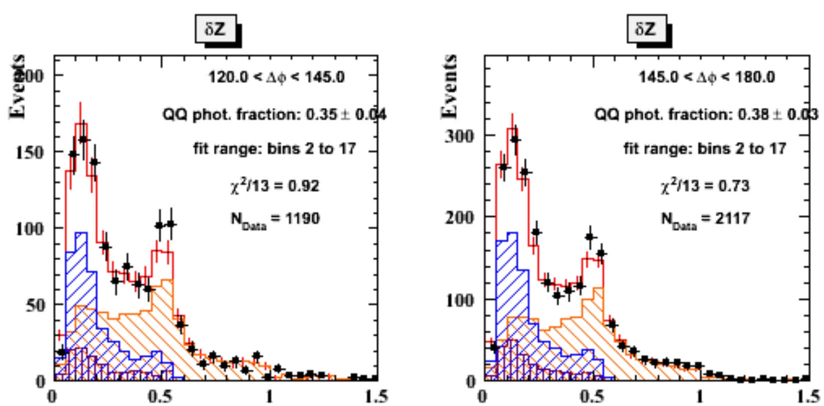

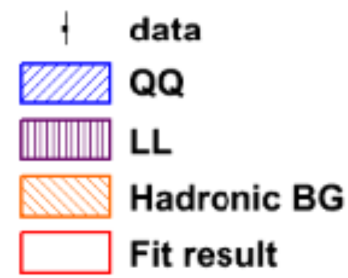

For **data = LL' + QQ' * a + bg' * (1-a)**
fitting with Ian's correction .

Across all the types of fitting the differences in calculated parameters are ~1-2%

Appendix. Comparison of fits

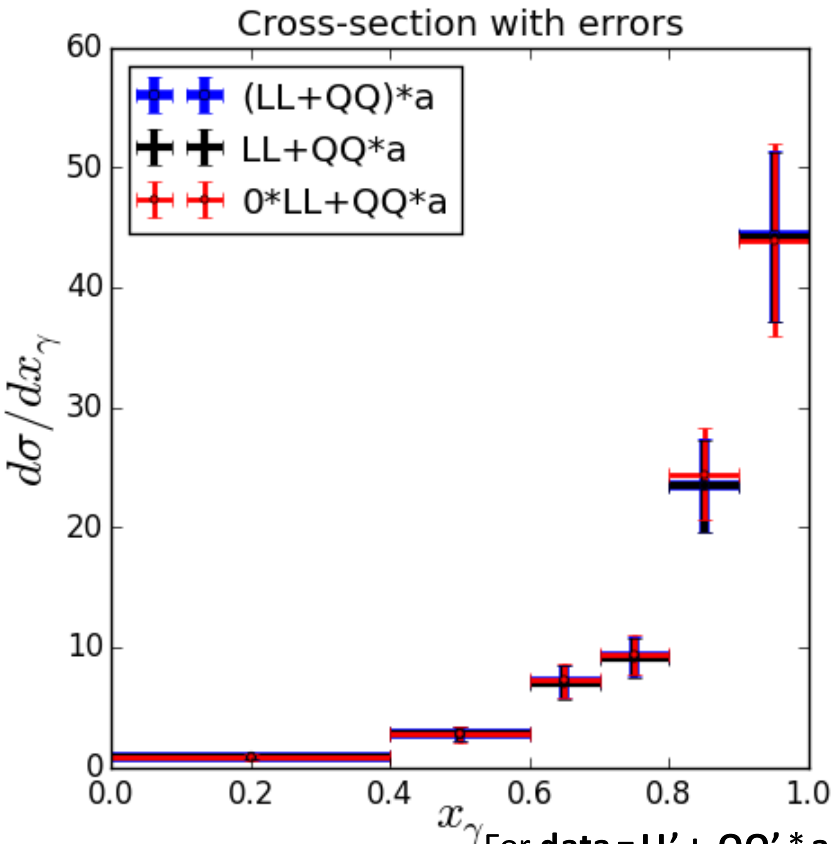

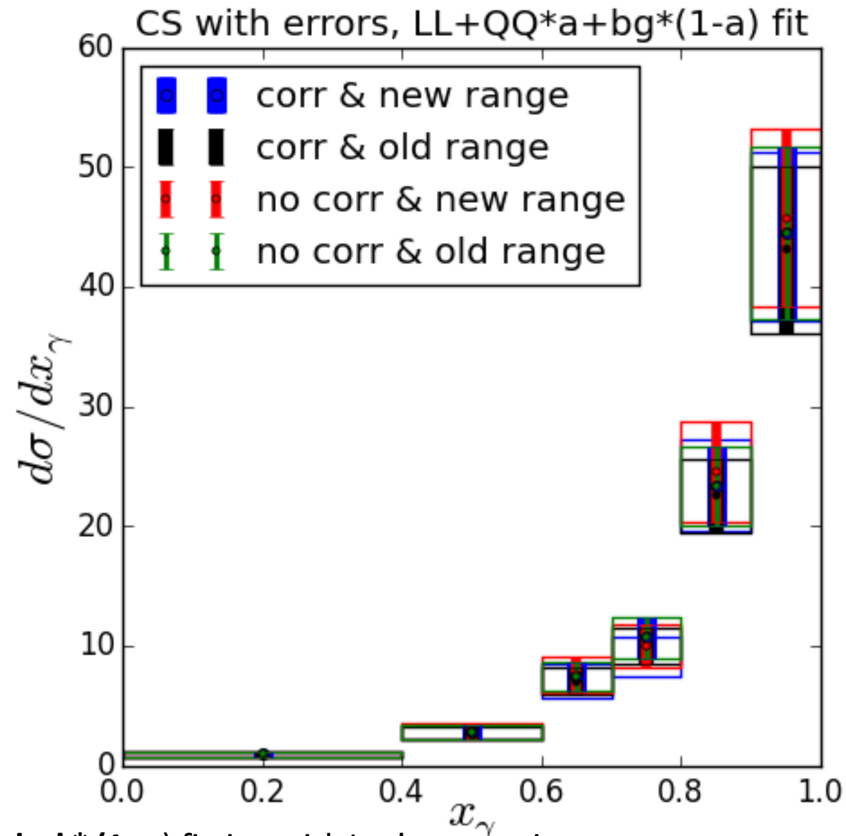

For **data = LL' + QQ' * a** + **bg' * (1- a**) fitting with Ian's correction .